NJC

PAPER

View Article Online
View Journal | View Issue

Published on 11 November 2019. Downloaded by Northwestern University on 1/3/2020 12:04:25 AM.

Check for updates

Cite this: *New J. Chem.*, 2019, **43**, 19331

Ag–NHC anchored on silica: an efficient ultra-low loading catalyst for regioselective 1,2,3-triazole synthesis†

Anirban Garg,[a] Nagesh Khupse,[b] Ankur Bordoloi[c] and Diganta Sarma*[a]

Received 26th July 2019,
Accepted 10th November 2019

DOI: 10.1039/c9nj03892b

rsc.li/njc

A silica-supported silver complex, Ag–NHC@SiO$_2$, was prepared by an anchoring coordination technique, which was successfully employed for the click reaction under mild reaction conditions. The protocol offered the remarkable advantages of operational simplicity, water as a reaction medium, ultra-low loading of the metal and easy recovery of the supported catalyst.

The azide–alkyne cycloaddition (AAC) reaction, popularly known as the click reaction, has been a promising tool for drug discovery, molecular biology and proteomic applications.[1] The original Huisgen cycloaddition of organic azides and alkynes can be successfully applied for triazole synthesis but has been found to have several demerits, such as the requirements of long reaction times and high temperatures as well as the lack of control in the regiochemical outcome of the product. However, the introduction of a Cu(I) catalyst rejuvenates this reaction to accomplish regioselectivity in a short reaction time.[2] Since then, the concept of click chemistry has been widely utilized in every field of chemistry. After the successful application of Cu catalysts, attempts have also been made by several researchers to replace copper, due to its cytotoxicity, with other metals such as ruthenium,[3] zinc,[4] iridium,[5] nickel,[6] and palladium.[7] Silver sources in various forms have long been used in different chemical transformations, like the synthesis of furan and its derivatives,[8] the total synthesis of (+)-asimicin and pyrroloistatin,[9] and the dearomatizing spirocyclization of alkyne-tethered aromatics.[10] The possibility of silver acting as a substitute to copper in AAC has been demonstrated by McNulty and coworkers[11] using P,O-type silver complexes for the first time, while Tuzun *et al.* provided mechanistic insights to the reaction through DFT studies.[12] In addition, Ag-based complexes,[13] Ag nanoparticles supported on graphene,[14] Al$_2$O$_3$@Fe$_2$O$_3$,[15] ceria,[16] and AgCO$_3$ in micellar media[17] have been employed successfully in AAC. Although there are a few reports on Ag-catalyzed azide–alkyne cycloaddition (AgAAC), there is a possibility for further improvements.

N-Heterocyclic carbenes (NHC) have become a popular choice of ligands for organic and inorganic chemists in synthesizing highly efficient homogeneous catalysts ever since Arduengo and co-workers isolated the first stable N-heterocyclic carbene (NHC) in 1991.[18,19] With strong σ-donation and weaker π-acceptor properties, NHCs can stabilize metal centres and hence are capable of forming complexes with almost all transition metals and many main group elements.[20] Attributing to these properties, metal NHCs are being used in different key catalytic steps of various organic transformations such as hydrosilylation of carbonyl compounds, intra and intermolecular C–H bond activation, and regioselective azide–alkyne 1,3-dipolar cycloaddition reactions.[21] Silver–NHC compounds are effective NHC transfer agents owing to their straightforward synthesis, avoiding the requirement for free NHC isolation and the relative stability of the Ag–NHC complexes towards light and air.[22] However, the use of these catalysts in aqueous media is quite limited.

The heterogenization of homogenous catalysts has evolved as an attractive tool to acquire recoverable and reusable catalysts. Although heterogeneous catalysts lack the distinct selectivity offered by homogeneous catalysts, they are indeed beneficial considering the depletable nature, complicated recycling problems and metal contamination of the products associated with homogeneous catalysts. Silica remains a popular choice of support to prepare heterogeneous catalysts owing to its easy availability, low cost and excellent porosity. The use of silica-supported catalysts in triazole syntheses has been well explored; however, the existing methods demand the use of high temperatures, organic solvents, longer reaction times or a high loading of the catalysts.[10,23] To the best of our knowledge, there is no report using silica-supported Ag–NHC complexes as catalysts for the click reaction let alone in aqueous media. In the search of an effective methodology for Cu-free click reactions, herein, we reported an ultra-low loading of an Ag(I)–NHC complex supported on silica as an efficient heterogeneous

---

[a] *Department of Chemistry, Dibrugarh University, Dibrugarh – 786004, Assam, India. E-mail: dsarma22@gmail.com*
[b] *Center for Materials for Electronics Technology, Pashan Road, Pune – 411008, India*
[c] *Nano Catalysis, Catalytic Conversion and Process Division, CSIR – Indian Institute of Petroleum, Mohkampur, Dehradun 248005, India*

† Electronic supplementary information (ESI) available. See DOI: 10.1039/c9nj03892b

Published on 11 November 2019. Downloaded by Northwestern University on 1/3/2020 12:04:25 AM.

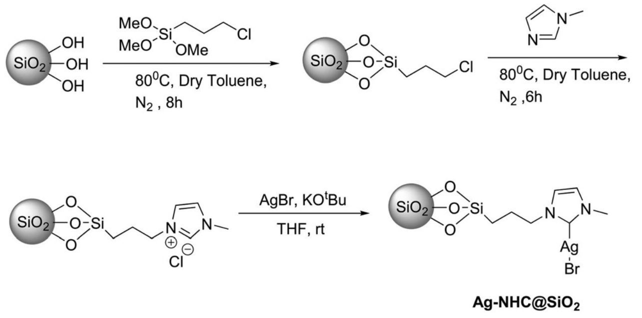

Scheme 1 Preparation of Ag–NHC@SiO$_2$.

catalyst for the regioselective synthesis of triazoles in water under ambient conditions.

Materials and methods

The preparation of Ag–NHC@SiO$_2$ was performed by a three-step procedure (Scheme 1) following the report by Lei Wang *et al.* for the synthesis of a silica-immobilized Ag–NHC complex for the A^3-coupling reaction.[24] The supported catalyst was prepared from commercial chromatography grade silica gel (60–120 Mesh), which was first functionalized with imidazole-based ionic liquids by the reaction with (3-chloropropyl)trimethoxysilane and then with 1-methyl imidazole in refluxing dry toluene for 8 h under a nitrogen atmosphere to obtain a silica-immobilized ionic liquid. After filtration and drying of the functionalized silica support, it was treated with AgBr in the presence of KO^{t}Bu in THF under light protection, which was again filtered and dried to obtain Ag–NHC@SiO$_2$ as a light grey coloured solid.

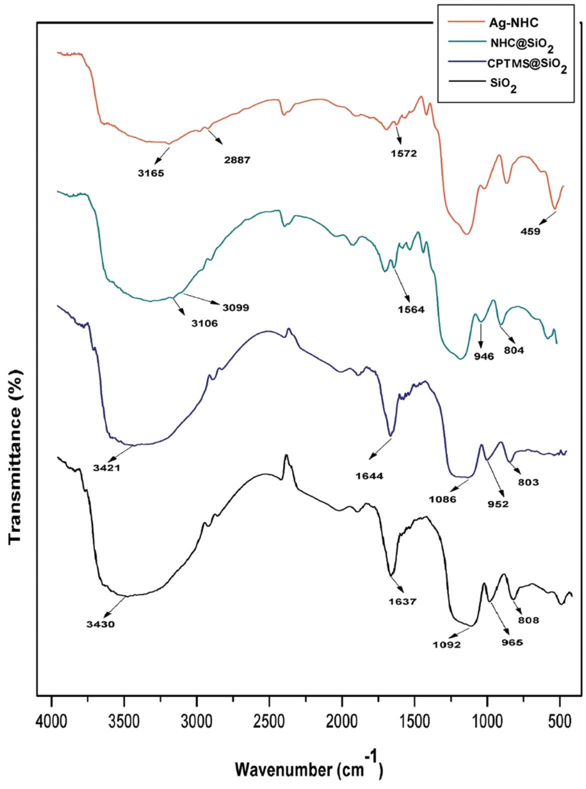

Fig. 1 FTIR spectra of various silica samples.

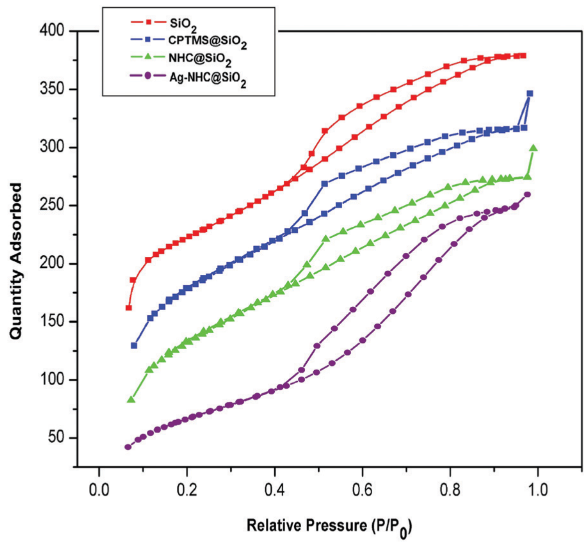

Fig. 2 N$_2$ adsorption–desorption isotherms of various silica samples.

Results and discussion

Ag–NHC@SiO$_2$ was characterized by FT-IR, TGA, SEM-EDX, and XRD. To validate the formation of the N-heterocyclic carbene complex and its effective immobilization on the silica surface, an infrared spectroscopic study was conducted. The FTIR spectra of the prepared samples are shown in Fig. 1.

For the samples, the bands around 1637 cm^{-1} and 3430 cm^{-1} can be ascribed to the νO–H stretching and bending vibrations of the adsorbed water, respectively. The absorption peaks observed around 808 and 1092 cm^{-1} were due to the Si–O–Si structure of the silica framework. A characteristic band at 965 cm^{-1} was found due to the silanol group of silica, indicating the formation of an –Si–O– bond, which was formed by the reaction of the silanol groups of silica with the (CH$_3$O)$_3$Si– group of CPTMS. However, after the functionalization of silica with CPTMS, 1-methyl imidazole and insertion of the metal, the intensity of this band progressively decreased for all the samples with each step due to a decrease in the availability of free silanol groups after the successful functionalization of the silica material. Comparing untreated silica with Ag–NHC@SiO$_2$, important features of the Ag catalyst were observed in the spectrum. The peaks at 3167 (sp^2 C–H stretching vibration of the imidazole moiety), 2887 (N–CH$_2$ stretching vibration) and 1572 cm^{-1} (C–N and C=C vibrations of the imidazole ring) clearly indicate the distinct attachment of all the materials and the successful attachment of the metal complex with the support.

N$_2$ adsorption–desorption is a common method to characterize porous materials, which can be helpful in providing insights into specific surface area, average pore diameter, pore volume, *etc.* The N$_2$ adsorption–desorption isotherms of various

Published on 11 November 2019. Downloaded by Northwestern University on 1/3/2020 12:04:25 AM.

Table 1 Surface area, pore size and volume distribution of the silica-based samples

Entry	Material	Surface area[a] (A_{BET}) (m^2 g^{-1})	Pore volume[b] (cm^3 g^{-1}) (V_p)	Pore diameter[c] (nm)
1	SiO_2	509.02	0.558	4.39
2	CPTMS@SiO_2	369.98	0.368	3.98
3	NHC@SiO_2	244.73	0.248	4.05
4	Ag–NHC@SiO_2	184.19	0.187	6.31

[a] BET method used in N_2 sorption. [b] Single-point pore volume at P/P_0 = 0.994. [c] Adsorption average pore diameter (by BET method).

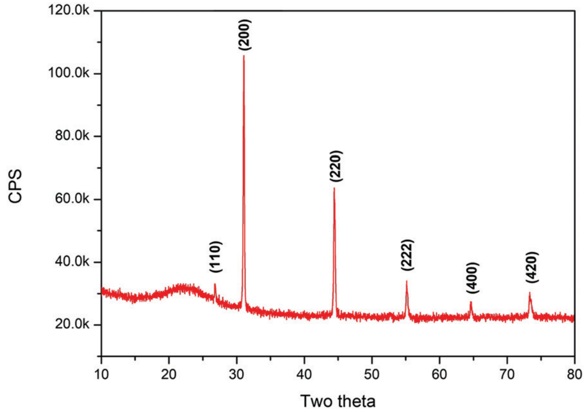

Fig. 3 Powder XRD image of the catalyst.

silica samples measured at 77.15 K are shown in Fig. 2. According to the IUPAC classification, all the samples are type IV with a typical hysteresis loop, featuring mesoporous materials with highly uniform pore size distribution.[25] The BET surface area, pore size and pore volume for different materials are presented in Table 1. The BET surface area for unfunctionalized SiO_2 was found to be 509.02 m^2 g^{-1}, while after functionalization with CPTMS and 1-methyl imidazole to generate silica-anchored NHC, a subsequent decrease in the A_{BET} value to 369.98 and 244.73 m^2 g^{-1} was observed, respectively.

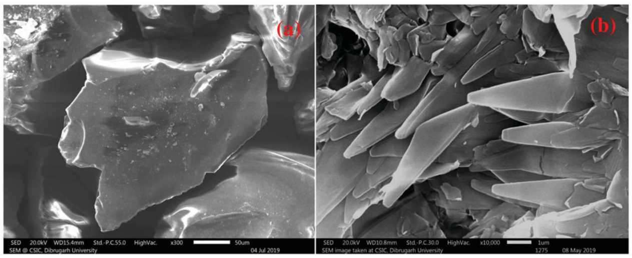

Fig. 5 SEM images of (a) silica and (b) Ag–NHC@SiO_2.

A further decrease in A_{BET} for the metal-immobilized silica sample to 184.19 m^2 g^{-1} is a clear indication of the successful anchoring of the Ag metal onto the functionalized support. Similarly, a gradual decrease in pore volume was observed from silica (0.558 cm^3 g^{-1}) to Ag–NHC@SiO_2 (0.187 cm^3 g^{-1}), further validating the formation of a silica-supported Ag–NHC complex.

Fig. 3 shows the X-ray diffraction pattern of Ag–NHC@SiO_2. It shows reflections at the 2θ values of 26.84, 31.04, 44.42, 55.15, 64.57 and 73.32, corresponding to the (110), (200), (220), (222), (400) and (420) planes of Ag; the reflection at 2θ of ∼22.4 was attributed to the silica component, indicating its amorphous nature.

The comparison of the EDX analyses (Fig. 4a and b) of silica with Ag–NHC@SiO_2 confirmed the presence of silver in the catalyst along with the other elements, indicating the formation of the desired metal complexes with the anchored ligand. The SEM images (Fig. 5a and b) of silica and the immobilized silver catalyst clearly indicate the changes in the morphologies of the catalyst after introduction of the metal.

Considering the results of ICP-AES and SEM-EDX, we could determine the attachment of the metal on the surface of the solid supports. The amount of the metal in the Ag–NHC@SiO_2 catalyst was determined by ICP-AES analysis and the loading of the metal was found to be 0.002 mmol g^{-1} of the catalyst (0.022 wt%). X-ray photoelectron spectroscopy (XPS) confirmed the presence of Ag(I) species along with other elements (Fig. 6). The binding energy of the O 1s component was found

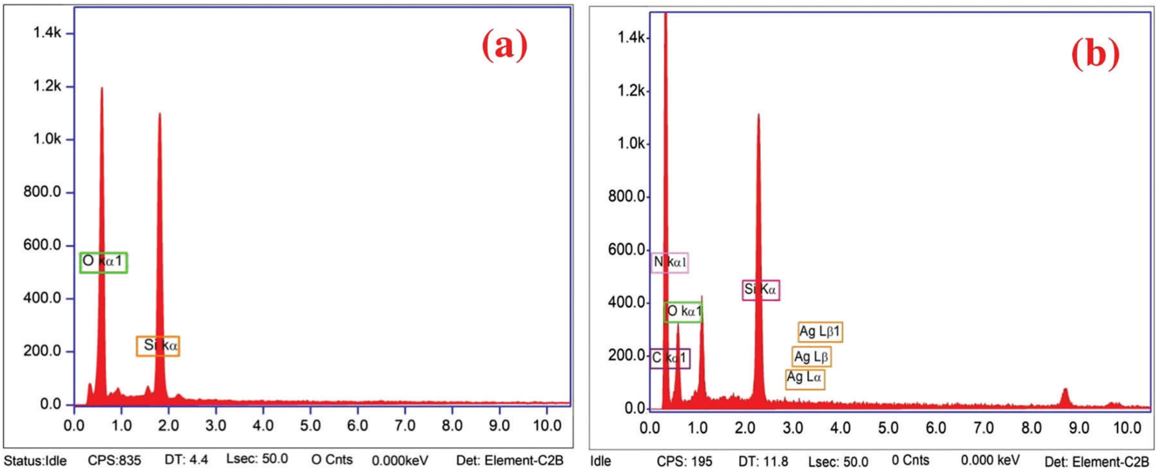

Fig. 4 SEM-EDX patterns of (a) silica and (b) Ag–NHC@SiO_2.

Published on 11 November 2019. Downloaded by Northwestern University on 1/3/2020 12:04:25 AM.

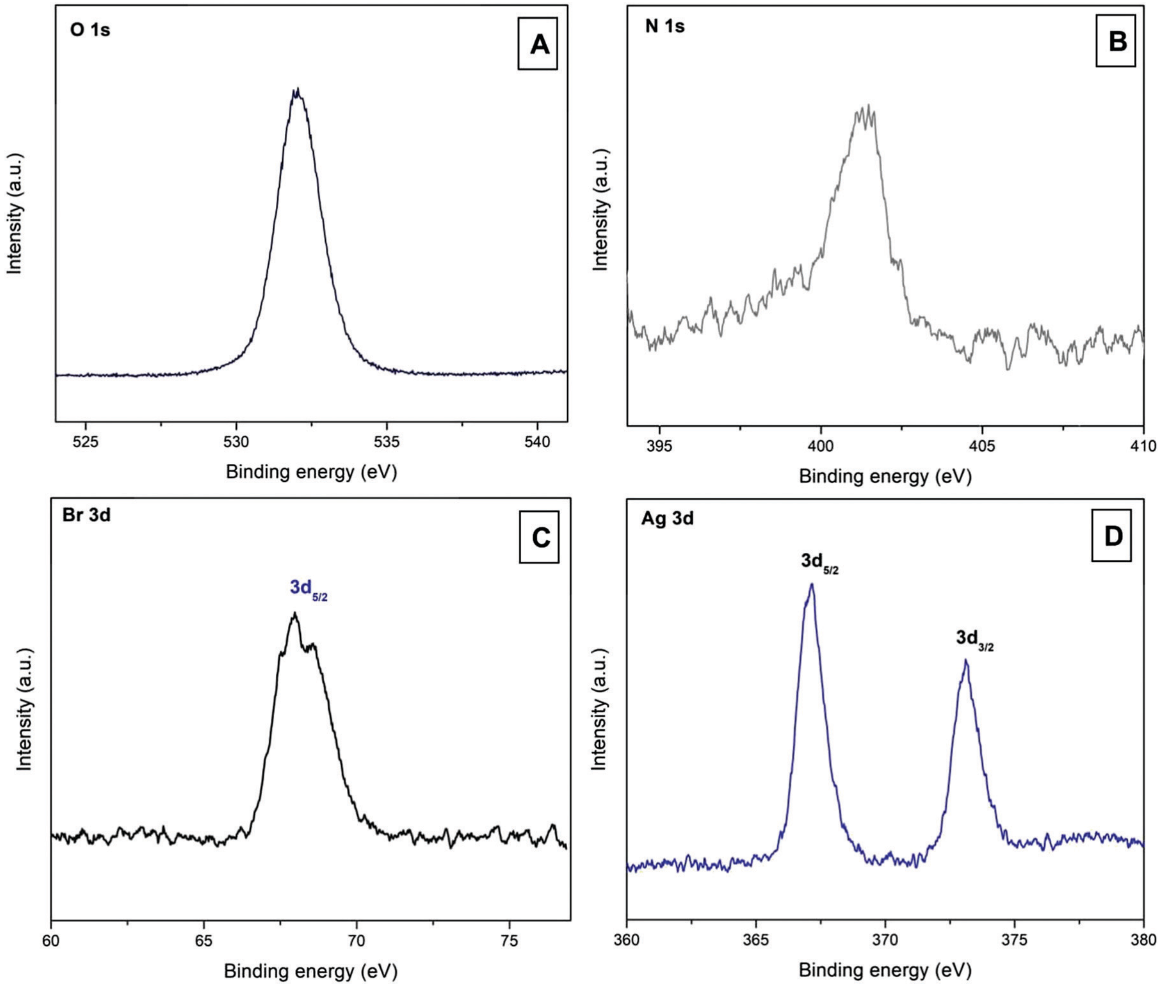

Fig. 6 XPS analysis of Ag–NHC@SiO_2 for (A) O 1s, (B) N 1s, (C) Br 3d, (D) Ag 3d.

to be 532.0 eV, which was obtained due to the presence of silica-bound silanol groups. The presence of the imidazole moiety even after incorporating Ag was validated from the N 1s curve (Fig. 6B), which had a peak at 401.3 eV. Similarly, the presence of Br was also confirmed by the Br 3d curve (Fig. 6C), exhibiting a peak due to the $3d_{5/2}$ component at 67.9 eV. Furthermore, the Ag 3d curve (Fig. 6D) could be fitted with peaks at the binding energies of 367.14 eV and 373.12 eV, corresponding to the $3d_{5/2}$ and $3d_{3/2}$ components for the Ag^+ oxidation state,[26] which was consistent with the formation of a silica-bound Ag–NHC complex.

The transmission electron microscopy images (Fig. 7) show a well dispersed distribution of spherical Ag–NHC@SiO_2 nanoparticles with a diameter of about 45.7 nm. The SAED diffraction pattern (Fig. 7d) indicates the amorphous nature of our catalyst.

To examine the thermal stability of the catalyst, thermogravimetric analysis (TGA) was performed from 35 to 880 °C at a ramp rate of 20 °C min^{-1} with a PerkinElmer STA 8000 instrument under nitrogen atmosphere (N_2 gas flow rate: 20 mL min^{-1}) with alumina as the reference. The TGA curve (Fig. 8) of the catalyst demonstrates the superior thermal stability of the catalyst up to 750 °C, indicating that it can be used over a wide temperature range for any chemical reaction.

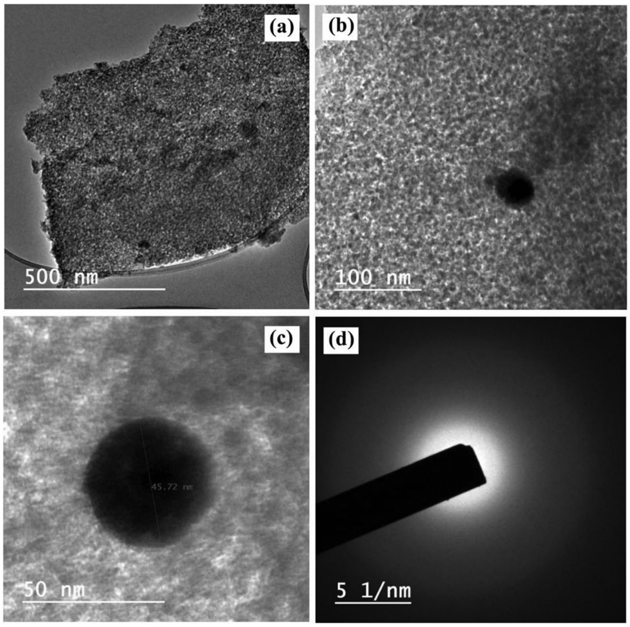

Fig. 7 (a–c) TEM images of Ag–NHC@SiO_2 at different magnifications; (d) SAED pattern of the catalyst.

Published on 11 November 2019. Downloaded by Northwestern University on 1/3/2020 12:04:25 AM.

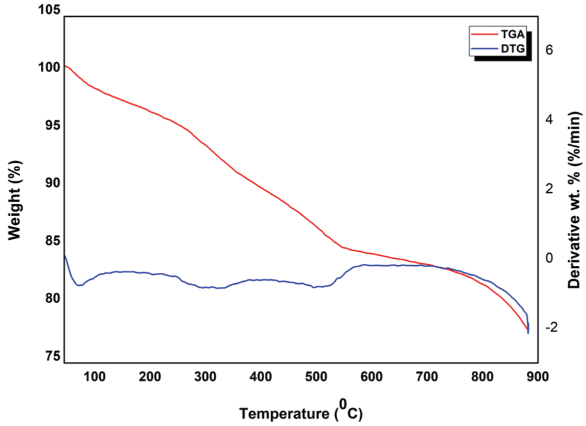

Fig. 8 TGA–DTG plot for the catalyst.

To investigate the catalytic performance of the Ag–NHC@SiO$_2$ catalyst towards azide–alkyne cycloaddition, benzyl azide and phenyl acetylene were chosen as the test substrates. The optimization studies are summarized in Table 2. Considering abundance and economic point of view, water was chosen as the medium to perform the click reaction with 15 mg catalyst at 60 °C and the reaction produced about 94% of the desired product in 6 hours. It was seen that a small amount of 1,5-regiomer was also produced along with the 1,4-disubstituted triazole, which encouraged us to further examine the feasibility of this protocol. The use of an additive is substantial to enhance the regioselectivity of this reaction; hence, we introduced different organic bases to study their effect in suppressing the formation of the 1,5-regiomer (Table 2, entries 2–5). In this context, quinine was found to produce the best result. We also changed the solvent from water to toluene as in the majority of the AgAAC reported, it is the solvent of choice. However, in our case, toluene turned out to be ineffective; DMF, THF, DMSO, EG, and binary solvent mixtures like water : DMSO (1 : 1), water : *t*-butanol (1 : 1), and water : CAN (1 : 1) failed to produce better results as well (Table 2, entries 6–13). It was also speculated that lowering the temperature as well as the catalyst loading largely affects the catalytic performance of the reaction, generating a lower product yield (Table 2, entries 14 and 15). The necessity of a catalyst was confirmed by a control experiment, which showed that in the absence of Ag–NHC@SiO$_2$, only a fraction of azide cyclized to triazole as a mere outcome of thermal dipolar cycloaddition with a clear lack of regioselectivity (Table 2, entry 16). Furthermore, it was confirmed that the Ag–NHC complex present in the supported catalyst was the active catalyst and the functionalized support without the metal played no role in initiating the reaction as no improvement was observed relative to the reaction performed without the catalyst when NHC@SiO$_2$ alone was used to promote cycloaddition (Table 2, entry 17). It is worth noting that the reaction also proceeded at room temperature although it required much longer time to achieve a reasonable yield.

To examine the general applicability and feasibility of transformation, various azides and alkynes were subjected to azide–alkyne cycloaddition reaction under similar conditions. The results are summarized in Table 3. Benzyl azide was found to be the

Table 2 Screening of solvent and additive for cycloaddition of benzyl azide (**1a**) to phenylacetylene[a]

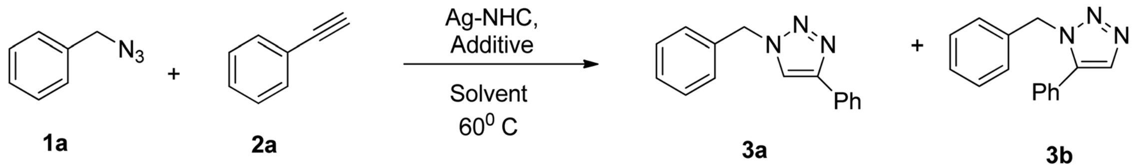

Entry	Solvent	Additive	Time (h)	Isolated yield **3a(3b)**
1	H_2O	—	6	79(15)
2	H_2O	DIPEA	6	90(5)
3	H_2O	Quinine	6	98(0)
4	H_2O	L-Proline	6	85(0)
5	H_2O	Xphos	6	60(35)
6	Toluene	Quinine	6	15(0)
7	DMF	Quinine	6	32(0)
8	THF	Quinine	6	22(0)
9	DMSO	Quinine	6	10(0)
10	EG	Quinine	6	31(0)
11	H_2O/DMSO (1 : 1)	Quinine	6	56(0)
12	H_2O/*t*-BuOH (1 : 1)	Quinine	6	60(0)
13	H_2O/ACN (1 : 1)	Quinine	6	27(0)
14	H_2O	Quinine	6	91[b](0)
15	H_2O	Quinine	6	89[c](0)
16	H_2O	—	6	12[d](10)
17	H_2O	Quinine	6	10(10)[e]
18	H_2O	Quinine	12	52[f](0)

[a] Reaction conditions: benzyl azide (0.5 mmol), phenyl acetylene (1.2 eq.), AgNHC 15 mg (0.006 mol%) with respect to benzyl azide, and additive (1 eq.) are stirred in 1 mL solvent at 60 °C. [b] Reaction mixture is stirred at 50 °C. [c] 12 mg of AgNHC was used. [d] Reaction carried out in the absence of catalyst and additive. [e] Reaction is carried out with NHC@SiO$_2$ instead of Ag–NHC@SiO$_2$. [f] Reaction is carried out at room temperature. Percentage of 1,5-regiomer is determined by GCMS.

Published on 11 November 2019. Downloaded by Northwestern University on 1/3/2020 12:04:25 AM.

Table 3 Scope of the catalytic system[a]

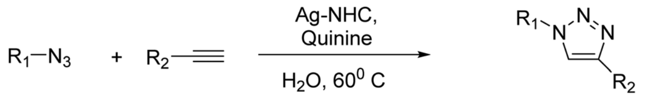

3a-3v

Entry	Azide (R_1)	Alkyne	Products	Time (h)	Yield[b] (%)	TON[c]	TOF[d] (h^{-1})
1	Benzyl (**1a**)	Phenyl acetylene	**3a**	5	98	8166	1633
2	Phenyl (**1b**)	Phenyl acetylene	**3b**	6	89	7416	1236
3	4-Chlorophenyl	Phenyl acetylene	**3c**	6	85	7083	1180
4	4-Fluorophenyl	Phenyl acetylene	**3d**	6	91	7583	1263
5	4-(Difluoromethoxy)phenyl	Phenyl acetylene	**3e**	6	85	7083	1180
6	3-Chlorophenyl	Phenyl acetylene	**3f**	6	92	7666	1277
7	2-Methylphenyl	Phenyl acetylene	**3g**	6	90	7500	1250
8	4-Nitrophenyl	Phenyl acetylene	**3h**	6	82	6833	1138
9	4-Cyanophenyl	Phenyl acetylene	**3i**	6	78	6500	1083
10	Octyl	Phenyl acetylene	**3j**	6	91	7583	1263
11	**1a**	2-Ethynyl-6-methoxynaphthalene	**3k**	6	87	7250	1208
12	**1a**	1-Iodo-4-(prop-2-yn-1-yloxy)benzene	**3l**	5	98	8166	1633
13	**1a**	1-Ethynyl-4-methoxy-2-methylbenzene	**3m**	6	75	6250	1041
14	**1a**	Propargyl alcohol	**3n**	6	91	7583	1264
15	**1a**	Ethyl propiolate	**3o**	6	93	7750	1291
16	**1b**	Propargyl benzoate	**3p**	6	91	7583	1264
17	**1b**	Propiolic acid	**3q**	6	61	5083	847
18	**1b**	Dimethylacetylene dicarboxylate	**3r**	6	94	7833	1305
19	**1b**	Diethylacetylene dicarboxylate	**3s**	6	92	7666	1277
20	**1b**	1-Hexyne	**3t**	5	90	7500	1500
21	**1b**	1-Octyne	**3u**	5	95	7916	1583
22	**1b**	3-Ethynylthiophene	**3v**	6	87	7250	1208

[a] Reaction condition: azide (0.5 mmol), alkyne (1.2 eq.), quinine (1 eq.), AgNHC 15 mg (0.006 mol%) with respect to azides are stirred in 1 mL solvent at 60 °C. [b] Isolated yields. [c] mmol of product per mmol of catalyst. [d] TON per unit time.

easiest to cyclize, while aromatic azides also reacted efficiently. It was seen that all the aromatic azides with electron-donating substituents reacted efficiently, affording the desired triazoles in good to excellent yields (Table 3, entries 2–7). The position of the substituents do not at all affect reactivity. However, aromatic azides with strong electron-withdrawing groups (Table 3, entries 8 and 9) were found to react sluggishly. Interestingly, octyl azide produced the corresponding triazole in a high yield (Table 3, entry 10). Similarly, the scope of alkyne substrates was also explored. It was observed that all alkynes irrespective of whether they were aromatic or aliphatic or contained diverse functionalities, *viz.*, acids, alcohols, esters, and ethers underwent a swift transformation to the desired products (Table 3, entries 11–21). Heterocyclic alkynes (Table 3, entry 22) also showed tolerance towards this protocol, reflecting the wide applicability of our catalytic system.

The excellent catalytic performance of the low-loading Ag catalyst may be attributed to the presence of the NHC ligand, which may have enhanced the stability of some intermediates like Ag-acetylide as well as the stability of the metal centre during the course of the reaction.[11b] In this context, the silica support also played an important role. Keeping in mind that the NHC complexes are not very stable, the support material indeed played a dominant role in terms of inducing the stability and compatibility of the NHC catalyst in water, which is rare.

Reusability of the catalyst

Reusability is a key factor in determining the potential of a heterogeneous catalyst. To study the reusability of our catalytic system, we examined the cycloaddition of benzyl azide and phenyl acetylene as a test reaction and the previously described optimized conditions were maintained throughout each cycle of reuse. For this purpose, after the completion of the reaction, the catalyst was first separated by simple filtration, washed alternatively with ethyl acetate and water for two cycles, dried and reused for subsequent runs. It was observed that the catalyst was reusable up to the 5th cycle with only a small decline in the catalytic performance (1st cycle 98% to 5th cycle 86%; Fig. 9). The slight decrease in yield may be due to a gradual physical loss during separation, filtration and washings between each run. The ICP-AES analysis of the

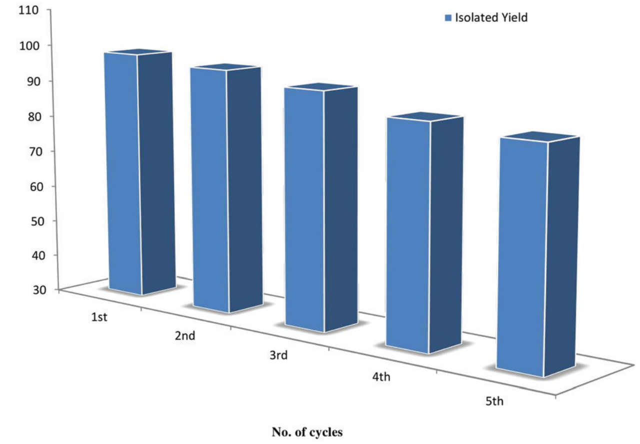

Fig. 9 Reusability of the catalyst.

Published on 11 November 2019. Downloaded by Northwestern University on 1/3/2020 12:04:25 AM.

reused catalyst revealed an extremely small amount of decrease in the metal loading. Furthermore, XRD analysis (ESI†) also showed almost no change in the diffraction pattern and the intensity of the peaks. These facts validate the strong anchoring of the NHC complex onto the silica surface.

Conclusion

In summary, an efficient, highly effective, low-loading silica-supported Ag–NHC catalyst was developed for the synthesis of triazoles through AgAAC. The method offered significant advantages over the existing methods employing silver catalysts in terms of broad substrate scope, easy handling, and most importantly ultra-low loading of silver metal, which could be reused for up to 5 cycles without losing its catalytic efficiency appreciably. Furthermore, water as a reaction medium and quinine as an additive contributed to the cleaner chemistry and greener credential of this protocol.

Conflicts of interest

There are no conflicts of interest to declare.

Acknowledgements

DS is thankful to DST, New Delhi, India for a research grant [No. EMR/2016/002345]. AG thanks DST, New Delhi for Research Fellowship. The financial assistance of DST-FIST and UGC-SAP programme to the Department of Chemistry, Dibrugarh University is also gratefully acknowledged.

References

1 P. Thirumurugan, D. Matosiuk and K. Jozwiak, *Chem. Rev.*, 2013, **113**, 4905–4979.

2 (*a*) C. W. Tornøe, C. Christensen and M. Meldal, *J. Org. Chem.*, 2002, **67**(9), 3057–3064; (*b*) V. V. Rostovtsev, L. G. Green, V. V. Fokin and K. B. Sharpless, *Angew. Chem., Int. Ed.*, 2002, **41**, 2596–2599.

3 (*a*) L. Zhang, X. Chen, P. Xue, H. H. Y. Sun, I. D. Williams, K. B. Sharpless, V. V. Fokin and G. Jia, *J. Am. Chem. Soc.*, 2005, **127**, 15998–15999; (*b*) L. K. Rasmussen, B. C. Boren and V. V. Fokin, *Org. Lett.*, 2007, **9**, 5337–5339; (*c*) B. C. Boren, S. Narayan, L. K. Rasmussen, L. Zhang, H. Zhao, Z. Lin, G. Jia and V. V. Fokin, *J. Am. Chem. Soc.*, 2008, **130**, 8923–8930.

4 (*a*) X. Meng, X. Xu, T. Gao and B. Chen, *Eur. J. Org. Chem.*, 2010, 5409–5414; (*b*) M. A. Morozova, M. S. Yusubov, B. Kratochvil, V. Eigner, A. A. Bondarev, A. Yoshimura, A. Saito, V. V. Zhdankin, M. E. Trusova and P. S. Postnikov, *Org. Chem. Front.*, 2017, **4**, 978–985.

5 E. Rasolofonjatovo, S. Theeramunkong, A. Bouriaud, S. Kolodych, M. Chaumontet and F. Taran, *Org. Lett.*, 2013, **15**, 4698–4701.

6 (*a*) H. S. P. Rao and G. Chakibanda, *RSC Adv.*, 2014, **4**, 46040–46048; (*b*) W. G. Kim, M. E. Kang, J. B. Lee, M. H. Jeon, S. Lee, J. Lee, B. Choi, P. M. S. D. Cal, S. Kang, J.-M. Kee, G. J. L. Bernardes, J.-U. Rohde, W. Choe and S. Y. Hong, *J. Am. Chem. Soc.*, 2017, **139**, 12121–12124.

7 J. Barluenga, C. Valděs, G. Beltrán, M. Escribano and F. Aznar, *Angew. Chem., Int. Ed.*, 2006, **45**, 6893–6896.

8 (*a*) J. A. Marshall and C. A. Sehon, *J. Org. Chem.*, 1995, **60**, 5966–5968; (*b*) S. J. Hayes, D. W. Knight, M. D. Menzies, M. O'Halloran and W.-F. Tan, *Tetrahedron Lett.*, 2007, **48**, 7709–7712.

9 (*a*) J. A. Marshall and K. W. Hinkle, *J. Org. Chem.*, 1997, **62**, 5989–5995; (*b*) D. G. Dunford and D. W. Knight, *Tetrahedron Lett.*, 2016, **57**, 2746–2748.

10 A. K. Clarke, M. J. James, P. O'Brien, R. J. K. Taylor and W. P. Unsworth, *Angew. Chem., Int. Ed.*, 2016, **55**, 13798–13802.

11 (*a*) J. McNulty, K. Keskar and R. Vemula, *Chem. – Eur. J.*, 2011, **17**, 14727–14730; (*b*) J. McNulty and K. Keskar, *Eur. J. Org. Chem.*, 2012, 5462–5470.

12 E. Boz and N. S. Tuzun, *Dalton Trans.*, 2016, **45**, 5752–5764.

13 (*a*) A. I. Ortega-Arizmendi, E. Aldeco-Pérez and E. Cuevas-Yañez, *Sci. World*, 2013, 1–8; (*b*) A. A. Ali, M. Chetia, B. Saikia, P. J. Saikia and D. Sarma, *Tetrahedron Lett.*, 2015, **56**, 5892–5895.

14 N. Salam, A. Sinha, A. Singha Roy, P. Mondal, N. R. Jana and S. M. Islam, *RSC Adv.*, 2014, **4**, 10001–10012.

15 P. Basua, P. Bhanjab, N. Salamc, T. K. Deya, A. Bhaumikb, D. Dasc and S. M. Islama, *Mol. Catal.*, 2017, **439**, 31–40.

16 S. Das, P. Mondal, S. Ghosh, B. Satpati, S. Deka, S. M. Islam and T. Bala, *New J. Chem.*, 2018, **42**, 7314–7325.

17 J. Sultana, N. D. Khupse, S. Chakrabarti, P. Chattopadhyay and D. Sarma, *Tetrahedron Lett.*, 2019, **60**, 1117–1121.

18 A. J. Arduengo, R. L. Harlow and M. Kline, *J. Am. Chem. Soc.*, 1991, **113**, 361–363.

19 *N-Heterocyclic carbenes in transition metal catalysis. Topics in organometallic chemistry*, ed. F. Glorius, Springer, Berlin, 2007, p. 21.

20 (*a*) J. Cheng, L. Wang, P. Wang and L. Deng, *Chem. Rev.*, 2018, **118**, 9930–9987; (*b*) Y. Wang and G. H. Robinson, *Inorg. Chem.*, 2014, **53**, 11815–11832.

21 (*a*) M. R. Fructos, P. de Fremont, S. P. Nolan, M. M. Diaz-Requejo and P. J. Perez, *Organometallics*, 2006, **25**, 2237–2241; (*b*) H. Kaur, Z. F. Kaur, E. D. Stevens and S. P. Nolan, *Organometallics*, 2004, **23**, 1157–1160; (*c*) S. Diez-Gonzalez, A. Correa, L. Cavallo and S. P. Nolan, *Chem. – Eur. J.*, 2006, **12**, 7558–7564.

22 (*a*) H. M. J. Wang and I. J. B. Lin, *Organometallics*, 1998, **17**, 972–975; (*b*) C. K. Lee, K. M. Lee and I. J. B. Lin, *Organometallics*, 2002, **21**, 10–12.

23 (*a*) S. Mohammed, A. K. Padala, B. A. Dar, B. Singh, B. Sreedhar, R. A. Vishwakarma and S. B. Bharate, *Tetrahedron*, 2012, **68**, 8156–8162; (*b*) T. Miaoa and L. Wang, *Synthesis*, 2008, 363–368; (*c*) L. Wan and C. Cai, *Catal. Lett.*, 2012, **142**, 1134–1140.

24 M. Wang, P. Li and L. Wang, *Eur. J. Org. Chem.*, 2008, 2255–2261.

25 S. Brunauer, L. S. Deming, W. E. Deming and E. Teller, *J. Am. Chem. Soc.*, 1940, **62**, 1723–1732.

26 (*a*) H. Xu, Y. Xu, H. Li, J. Xia, J. Xiong, S. Yin, C. Huang and H. Wan, *Dalton Trans.*, 2012, **41**, 3387–3394; (*b*) L. Kong, Z. Jiang, H. H. Lai, R. J. Nicholls, T. Xiao, M. O. Jones and P. P. Edwards, *J. Catal.*, 2012, **293**, 116–125.